Coupled Neutronics and Thermal Hydraulics Simulations of a BWR Fuel Channel in the Version5 Environment

Raphaël Guasch [1,*], Clément Huet[1], Alain Hébert[1], Cédric Béguin[1], Guy Marleau[1]

[1]Polytechnique Montréal, Montréal, Québec, Canada

ABSTRACT

Modeling Boiling Water Reactors (BWRs) in deterministic neutron transport codes presents significant challenges due to the substantial void fraction introduced in the coolant. This strong interdependence between neutron transport and thermal-hydraulics motivates the development of coupled multi-physics calculation schemes. This work presents progress made at Ecole Polytechnique de Montréal (EPM) in the modeling of BWRs in the Version5 environment. The DONJON5 full core solver is used to obtain an axial power distribution. The latter is then provided to our open source thermal-hydraulics (TH) solver. A single BWR fuel rod, both used as an equivalent full core and fuel channel, is selected as a simple comparison test case. Neutron transport and thermal-hydraulics calculations are compared to Serpent2 and GeN-Foam respectively. Work done towards numerically validating the newly implemented TH solver and the multi-physics iterative procedure is presented.

Keywords: Deterministic codes, multi-physics, neutron transport, thermal hydraulics.

1. INTRODUCTION

The strong multi-physics coupling observed in Boiling Water Reactors (BWRs) requires calculation routes capable of describing coupled thermal-hydraulics and neutron transport phenomena. Indeed, the axial voiding of the cooling water induces significant changes in the neutron transport properties[1]. Most notably, the coolant density decreases, causing a lack of thermalization of the neutron flux. This induces a loss of reactivity in the upper part of the fuel channel. The axial variation in the fuel effective temperature impacts the resonant absorption of neutrons due to Doppler broadening[2], also leading to a loss of reactivity in the upper section of the core.

The current `THM:`[3] module of DONJON5[4] has historically been developed to model CANDU and PWR designs. It is therefore not well suited to model two-phase flows encountered in BWRs. In this work, we present our new `THM prototype`, aimed at extending the capabilities of DONJON5 in terms of BWR thermal-hydraulics modeling. Our `THM prototype` solver consists of a stand-alone open-source Python3 program that can be found on the PolyBWR GitHub page. The open-source character of our `THM prototype` makes it a good candidate for future implementation in the DONJON5 full core code.

The presented solution is based on a drift flux model, which allows for the treatment of the convective heat transfer along a fuel channel. Additionally, the radial temperature distribution in the fuel and clad is solved for, providing us with an effective fuel temperature to be used in the neutronics solution.

*raphael.guasch@polymtl.ca

The thermal-hydraulics properties obtained with `THM prototype` can in turn be used to interpolate microscopic cross sections, used in the full core DONJON5 code to iteratively refine our estimate for the axial power profile.

Code-to-code comparisons are performed in order to assess the performances of our proposed coupled calculations route. The resulting axial power density of DONJON5 is compared to a reference Serpent2[5] solution. The DONJON5 power distributions are exported, allowing for a `THM prototype`-GeN-Foam[6] comparison. The numerical stability and convergence of the method are assessed by performing a spatial convergence study on the axial meshing parameters.

2. THEORY

The `THM prototype` is composed of two sub-modules, the first is responsible for solving the steady-state convective heat transfer problem at the coolant/clad interface. This includes solving for velocity, pressure, coolant temperature and void fraction along the channel. The second sub-module is used to solve for the thermal conduction in the cladding and the fuel. This provides a fuel temperature distribution, which can be used to estimate the effective fuel temperature for neutron transport applications.

2.1. Convection in the coolant

This new version of the module implements a homogeneous fluid, three-field representation (mixture velocity u_m, channel pressure p, and mixture enthalpy h_m) of two-phase flows. This enables it to model boiling and vapor formation in BWR channels. The `THM prototype` allows for the simulation of a 1D square or cylindrical channel flow. Each channel is characterized by 1D convection equations. The equations of mass, momentum and energy conservation are solved using an homogeneous drift flux model[7].

The mixture continuity, momentum and enthalpy-energy equations can be written as the following system of equations:

$$\frac{\partial}{\partial z}\left(A\rho_m u_m\right) = 0 \tag{1}$$

$$\frac{\partial}{\partial z}\left[\rho_m u_m^2 + \frac{\varepsilon}{1-\varepsilon}\frac{\rho_v\,\rho_\ell}{\rho_m}V_{vj}^2\right] + \frac{\partial}{\partial z}\,p + \rho_m g = -\frac{4\tau_w}{D} \tag{2}$$

$$\frac{\partial}{\partial z}\left[\rho_m u_m h_m\right] + \frac{\partial}{\partial z}\left[\varepsilon\frac{\rho_v\rho_\ell}{\rho_m}V_{vj}(h_v - h_\ell)\right] = \frac{\partial}{\partial z}p \cdot \left[u_m + \frac{\varepsilon(\rho_l - \rho_g)}{\rho_m}V_{vj}\right] + \vec{n}_w \cdot \vec{q}''_w \tag{3}$$

To close the system of equations, constitutive relations are needed to model the thermal behavior of the flow. The `THM prototype` implements correlations for void fraction, friction losses, drift velocity and equation of states to determine the density and other steam/water properties. The void fraction ε is determined using the standard drift flux model equation based on the flow quality:

$$\varepsilon = \frac{x}{C_0\left(x + \frac{\rho_g}{\rho_\ell}(1-x)\right) + \frac{\rho_g V_{vj}}{\rho_m u_m}} \tag{4}$$

Symbols introduced in equations 1, 2, 3 and 4 are summarized in Table I.

The void distribution parameter and the drift velocity are computed using the Electric Power Research Institute (EPRI) void model used in the PATHS/PARCS code[8].

Table I. Summary of Symbols

Symbol	Description	Symbol	Description
A	Flow area	x	Flow quality
ρ_m	Mixture density	C_0	Void distribution parameter
ρ_v	Vapor density	V_{vj}	Drift velocity
ρ_l	Liquid density	τ_w	Friction losses
h_v	Enthalpy of saturated vapor	g	Gravitational acceleration
h_l	Enthalpy of saturated liquid	D	Hydraulic diameter
h_m	Enthalpy of the mixture	$\vec{n}_w \cdot \vec{q}''_w$	Volumetric heat source

To solve equations 1, 2 and 3, a finite difference method is used and the equations are cast into a face-based scheme which is motivated by the use of the inlet and outlet Dirichlet conditions. This reduces the problem to a 1D flow with fixed inlet mass flow rate, inlet temperature and outlet pressure. First, the mass and momentum equation are solved simultaneously across all nodes using the preconditioned Bi-conjugate Gradient (BiCG) method. Then, the energy conservation equation is solved using the updated velocity and pressure fields. As the inlet pressure is determined at each iteration and the flow rate and the temperature remains constant, the inlet velocity and inlet enthalpy are adjusted. This step ensures a consistent pressure drop along the channel. The new velocity, pressure and enthalpy fields are then used to compute state variables and drift flux parameters. An iterative process is used due to the coupling between the void fraction correlation and the density of the mixture.

2.2. Conduction in the fuel pin

The Fourier law of heat conduction models the temperature distribution in the fuel rod. A radial symmetry of the temperature distribution is assumed. The fuel rod is meshed according to a *constant surface* discretization. The heat conduction equation is solved using a mesh-centered finite difference method (MCFD). Boundary conditions at the fuel surface and gap/cladding surface ensure continuity of the heat flux. Due to the coupling between the surface heat exchange coefficient and the coolant temperature, the latter is iteratively updated until convergence is reached. Further details of the method are referenced in Héberts's documentation[3]. As stated earlier, the conduction solver implemented in our `THM prototype` is limited to constant, temperature independent thermal transfer properties presented in Table II. Once the temperature distribution has been obtained, the effective fuel temperature T_F is computed using Rowland's formula[3].

3. METHODOLOGY

Homogenized and condensed cross sections are obtained using the DRAGON5 lattice code. The DONJON5 finite core code is used to perform diffusion calculations on a single fuel channel. The neutron transport properties are assumed to be homogeneous in each axial node. As the coolant void fraction, density and fuel effective temperature vary, a *linear* interpolation of microscopic cross sections is performed, associating new material properties to each fuel bundle. The temperature and density values used in the diffusion solution are obtained via our `THM prototype`. The coupling between neutronics and TH fields is ensured through a *PyGan* script described in section 3.4. DONJON5 to Serpent2 and `THM prototype` to GeN-Foam comparisons are performed. Numerical validation criteria are set.

3.1. Problem specifications

The geometry of the problem is that of a single ATRIUM-10 pin cell[9]. At the lattice calculation step, the fuel pellet is radially divided into four radial regions to account for spatial self-shielding effects. Each

of these represents 50, 30, 15 and 5 % of the total fuel volume. The fuel composition is UOX at 2.4% enrichment.

BWR core representative data has been obtained from [10]. The selected user input geometrical, thermal hydraulics and heat transfer properties are shown in Table II. The total rod height is taken from a GeN-Foam test case[11]. It is worth noting that the thermal conductivity values for the fuel, clad and the convective heat transfer coefficient at the gap are set. The tests are carried out for total powers of $P_{tot} = 10$ and $35kW$.

Table II. Specifications of the case studied : geometric features, thermal-hydraulic data, and heat transfer properties.

Specifications of the studied case			
Thermal-hydraulic properties	**Value**	**Geometric data**	**Value**
Inlet temperature (K)	$T_{in} = 543.15$	Channel pitch (cm)	$p_c = 1.295$
Outlet pressure (MPa)	$P_{out} = 7.2$	Fuel radius (cm)	$r_f = 0.4435$
Mass flow rate (kg/s)	$\dot{m} = 8.407 \times 10^{-2}$	Cladding radius (cm)	$r_c = 0.514$
Hydraulic diameter (cm)	$D_h = 1.049$	Channel length (m)	$h = 1.555$
Heat transfer properties			
Fuel thermal conductivity (W/mK): $k_{fuel} = 4.18$			
Gap heat exchange coefficient (W/m^2K): $H_{gap} = 10000$			
Cladding thermal conductivity (W/mK): $k_{clad} = 21.5$			

3.2. Generating microscopic cross sections : the DRAGON5 lattice code

A two-steps lattice scheme is used to obtain spatially homogenized and group condensed microscopic cross sections using the SHEM[12] 295 energy groups based on the JEFF3.1.1 library. The 2 groups condensed and homogenized cross sections are tabulated as a function of three parameters: effective fuel temperature T_F, coolant temperature T_m and coolant density ρ_m. For every tabulation point, a self-shielding calculation is performed using the newly implemented RSE method[13]. The main flux calculation is performed using the method of characteristics (MOC). A specular reflective boundary condition is enforced. It is worth noting that at this stage, no leakage or reflector models have been introduced. Table III shows the T_F, T_m and ρ_m values for which microscopic cross sections were obtained and indexed in the `MULTICOMPO` object.

Table III. Tabulation points for T_F, T_m, ρ_m, used in lattice calculations.

Parameter	**List of tabulation points**
Effective fuel temperature T_F (K)	500, 700, 900, 1100, 1300, 1500, 1800
Coolant temperature T_m (K)	500, 540, 550, 560, 570
Coolant density ρ_m (kg/m^3)	10, 100, 200, 300, 400, 500, 600, 700, 800

3.3. Full core diffusion calculations in DONJON5

The equivalent "full core" geometry is defined in the DONJON5 code. Reflective boundary conditions are imposed at the $\pm X$ and $\pm Y$ limits. Void boundary conditions are enforced at the top and bottom Z surfaces. The TRIVAC5 [14] finite elements solver is used to perform a two-groups flux calculation in the diffusion theory. Cross sections for each axial fuel slice are obtained by linearly interpolating from the `MULTICOMPO` database produced by DRAGON5.

Table IV. Convergence criteria set for multi-physics iterations

Quantity	Convergence criteria
Nodal power	0.01 %
k_{eff}	0.1 pcm
Nodal T_F	0.001 K
Nodal T_m	0.001 K
Nodal ρ_m	0.001 kg/m^3

3.4. Steady state coupled neutronics-TH loop

Our algorithm aims at computing fields representative of the coupled neutronics-TH system. For each axial node, it computes the local power, fuel effective temperature, coolant temperature and density. The void fractions and power densities are also retrieved in each node along the axial dimension.

The implementation makes use of the Python3 *LCM* and *CLE-2000* APIs available through GANLIB Version5 [15]. The latter allows for the manipulation of DONJON5 procedures, *LCM* data structures as well as our `THM prototype` from a unique Python3 procedure.

The proposed coupling procedure is schematized as shown in Figure 1.

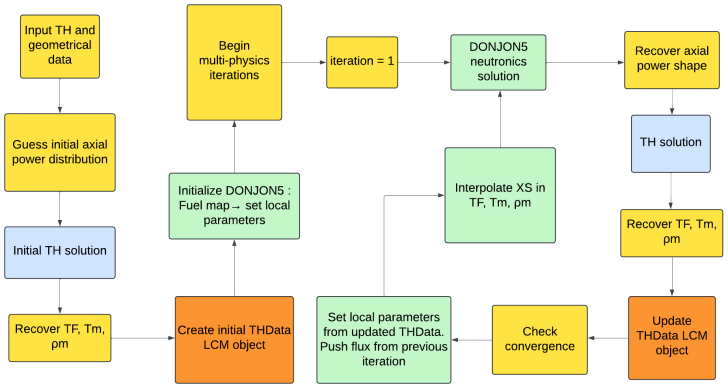

Figure 1. Multi-physics coupling loop : data flow in *PyGan* procedure. Steps performed in the main Python3 procedure, calls to our `THM prototype`, to the *Python3 LCM* API and to procedures through the *Python3 CLE-2000* API are respectively indicated by yellow, blue, orange and green boxes.

As an initial guess, a sinusoidal power distribution is assumed along the axial dimension. This allows us to initialize TH fields which can in turn be used to initialize the neutronics solver. Microscopic cross sections stored in the `MULTICOMPO` are interpolated in T_F, T_m and ρ_m. Each axial node has an associated material *mixture* with unique neutron transport properties. A two-groups diffusion theory flux calculation is then performed by the FEM solver TRIVAC5[14]. The computed power distribution is normalized to P_{tot}. Feeding this power distribution back into our `THM prototype` allows us to update the values of TH fields. This process is repeated iteratively until all convergence criteria on nodal power, T_F, T_m, ρ_m and k_{eff} are met. The convergence criteria for the coupled procedure are presented in Table IV.

3.5. Numerical verification and validation methodology

A first verification step is performed, checking the proper spatial convergence of our coupled calculation. Then, a code-to-code comparison is performed in an attempt to validate both our neutronics and thermal-

hydraulics solutions. Converged fields are exported and used to run independent reference neutronics and thermal-hydraulics calculations.

The converged T_F, T_m and ρ_m fields are used to set-up an exact geometry 3D Serpent2[5] model of the pincell. Detector scores for total heat production (MT=301) are extracted from each axial slice. In order to ensure statistical convergence, 10^4 batches of 5×10^4 neutrons are simulated, discarding the first 500 generations. To allow for a direct DONJON5-Serpent2 comparison of power distributions, the latter are normalized to the same total power used in the DONJON5 solution.

The converged power density distribution is also exported to set up an equivalent two-phase flow problem in GeN-Foam[6]. GeN-Foam is a computational tool based on OpenFoam, developed for reactor analysis. It specializes in the modeling of thermal-hydraulic processes using a two-fluid, three field representation of the two-phase flow.

The water temperature T_m, pressure P and void fraction ε are compared to GeN-Foam reference field using Root-Mean-Squared (RMS) deviations to determine their associated errors. Since GeN-Foam treats liquid and vapor phases distinctly, the equivalent mixture temperature is computed using : $T_m = \varepsilon T_v + (1 - \varepsilon T_l)$.

For this prototypal coupled calculation scheme to be considered valid we set the following criteria :

1. DONJON5 succeeds at providing a power density distribution with a RMS relative deviation (D5-S2) below 3%.
2. DONJON5 computes a k_{eff} value within a $\pm 150 pcm$ range of Serpent2.
3. DONJON5 nodal errors on power distributions stay withing a ±5% interval from Serpent2.
4. `THM prototype` successfully provides void fraction and coolant temperature distributions with RMS (THM-GeNFoam) relative deviations below 5%.

4. NUMERICAL RESULTS AND ANALYSIS

4.1. Coupled neutronics-TH loop verification

Coupled neutronics-TH calculations are performed using the EPRI void fraction correlation[8], the Churchill[16] correlation for the friction factor and the Lockhart-Martinelli[17] correlation for the pressure drop. Total power normalizations to $10kW$ and $35kW$ are compared. The resulting power density, fuel temperature, coolant temperature, coolant density and void fraction distributions are studied for varying axial meshes. Figures 2a and 2b respectively show power density and void fraction distributions along the fuel channel. computed on meshes with 40 and 160 nodes.

In order to assess the spatial convergence of our solution, TH fields computed on the coarser meshes are compared to those obtained on the finest 160 nodes mesh. Field values are associated to the mid points of control volumes, reference values are obtained by linearly interpolating between the 160 reference values. The RMS deviations on nodal error distributions are computed for fuel and coolant temperatures, coolant densities and void fractions. Table V displays the RMS deviations (Δ_{RMS}) evolution as the number of axial mesh elements increases. The spatial convergence of our solution acts as a verification of the self-consistency of the method.

4.2. Validation of the neutronics solution

The D5-S2 deviations on k_{eff} are shown in Table VI. RMS and nodal D5-S2 deviations on normalized power distributions are plotted in Figures 3a and 3b. The horizontal red lines indicate criteria set for a DONJON5 calculation to be validated. As seen in Table V, the agreement of $\pm 150 pcm$ on Δk_{eff} is reached for all meshes for $P_{tot} = 10kW$ and for all meshes with $n \geq 20$ for $P_{tot} = 35kW$. It can be seen from 3a that

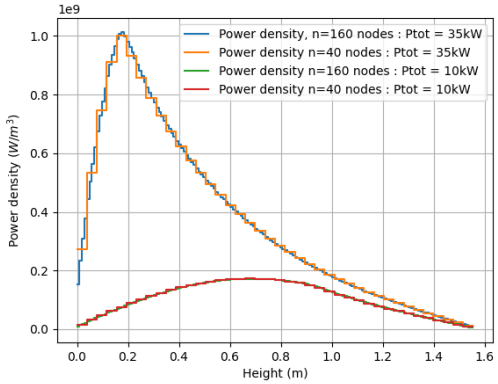

(a) Axial power density distribution.

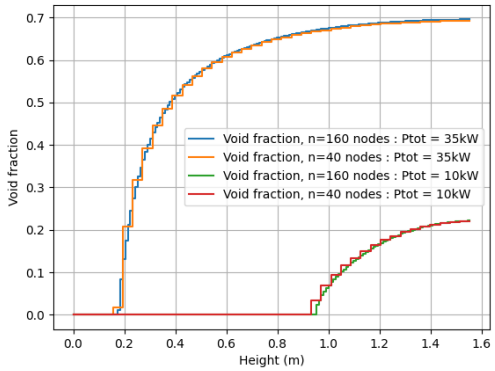

(b) Void fraction evolution in the fuel channel.

Figure 2. Power density (a), void fraction (b) evolution along the axial direction. Spatial convergence analysis for increasingly fine meshes. Power normalizations $10kW$ and $35kW$.

Table V. Dependence of Δ_{RMS} on axial mesh discretisation for 10 kW and 35 kW power normalizations.

Axial mesh	$\Delta_{RMS}\ T_F$ (K)		$\Delta_{RMS}\ T_m$ (K)		$\Delta_{RMS}\ \rho_m\ (kg/m^3)$		$\Delta_{RMS}\ \varepsilon$ (%)	
	10 kW	35 kW	10 kW	35 kW	10 kW	35 kW	10 kW	35 kW
10	1.12	13.6	0.59	1.56	6.15	38.1	8.80	5.44
20	1.21	6.48	0.41	0.38	4.13	8.36	5.91	1.19
40	0.71	3.60	0.21	0.19	3.02	3.01	4.33	0.43
70	0.32	2.37	0.10	0.09	1.26	1.59	1.79	0.23
80	0.23	1.98	0.07	0.07	0.85	1.79	1.22	0.25

Table VI. Evolution of Δk_{eff} (pcm) with increasing number of axial slices for power levels 10kW and 35kW.

Number of Axial Nodes	**Δk_{eff} (pcm) at 10kW**	**Δk_{eff} (pcm) at 35kW**
10	97	406
20	79	148
40	69	87
70	75	71
80	71	73
160	68	71

cases with $n > 40$ axial nodes successfully meet the 3% requirement set for the Δ_{RMS} on the power density distribution. Furthermore, Figure 3b shows that except for nodes close to the $\pm Z$ boundaries, the nodal errors for axial meshes $n = 70$ and $n = 160$ meet the ±5% criteria on D5-S2 deviations. The over estimation of D5 rates at $\pm Z$ boundaries can be explained by the choice of void boundary conditions. The latter induce a steep gradient in the neutron flux, which introduces numerical approximations in the FEM implementation of the "zero re-entrant angular flux"[18] condition. Additionally, the low neutron flux in such regions leads to more important variances associated with S2 scores tallied close to the boundary, which contributes to the increase in nodal errors close to the $\pm Z$ boundaries. It is hypothesized that this effect could be mitigated by introducing an axial reflector model. It should be noted that the error distributions for the $P_{tot} = 35kW$ case depend on z. This is explained by neutron axial streaming effects due to the more important void fractions in the upper sections of the channel.

The D5-S2 comparison shows that the presence of important void fractions requires a fine axial mesh to properly represent axial power variations. The $n = 70$ axial mesh is therefore selected for the `THM prototype` - GeN-Foam comparison.

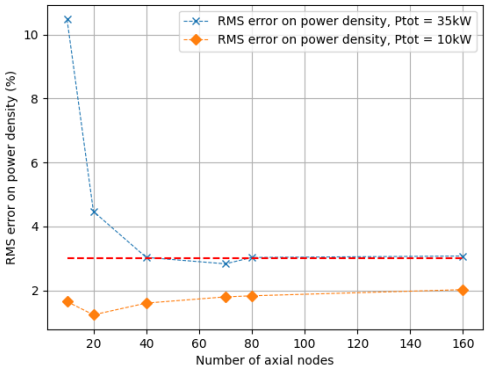

(a) D5-S2 Δ_{RMS} (%) on power density. Cases for $n = 10, 20, 40, 50, 70, 80$ and 160 axial nodes are presented.

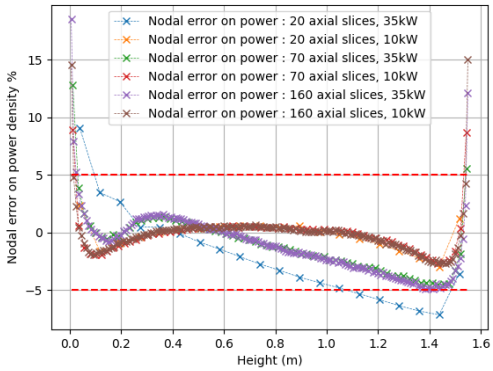

(b) Nodal (%) D5-S2 deviation on power density distributions. Cases for $n = 20, 70, 160$ axial nodes and $P_{tot} = 10kW, 35kW$ are presented.

Figure 3. D5-S2 RMS deviation between power density distributions (a) and axial evolution of nodal relative deviation on power densities (b).

4.3. Comparison of `THM prototype` solution to GeN-Foam

Figure 4 presents comparisons of our `THM prototype` to the GeN-Foam solution for cases with $P_{tot} = 10kW$ and $35kW$. The axial evolutions of the void fractions, pressures, and coolant temperatures are compared. It is important to note that GeN-Foam offers a two-phase description of the flow that inherently introduces differences with respect to our equivalent `THM prototype` mixture.

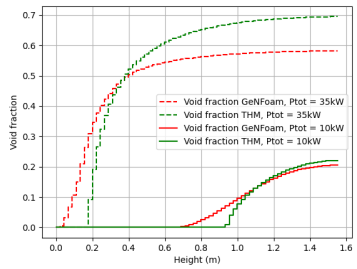

(a) Void fraction.

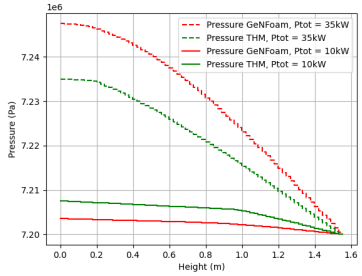

(b) Pressure.

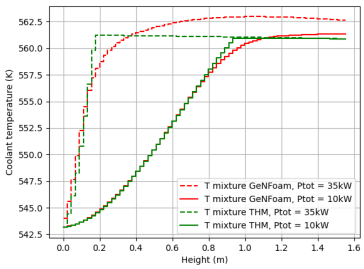

(c) Coolant temperature.

Figure 4. Void fraction (a), pressure (b), and coolant temperature (c) evolution along the axial dimension. Full and dashed lines respectively correspond to the $P_{tot} = 10kW$ and $P_{tot} = 35kW$ cases. The green and red colors are associated to the `THM prototype` and to the GeN-Foam solutions respectively.

Table VII shows the RMS (Δ_{RMS}), the average (Δ_{avg}) and maximum (Δ_{max}) deviations obtained when comparing `THM prototype` and GeN-Foam distributions obtained for ε and p and T_m. The errors on the predicted pressure drops are $4kPa$ and $-11kPa$ for the $10kW$ and $35kW$ cases respectively.

Table VII. Absolute RMS, maximum, and average `THM prototype`-GeNFoam deviations on pressure, void fraction and coolant temperature at power levels 10kW and 35kW.

Physical quantity	Δ_{RMS}		Δ_{max}		Δ_{avg}	
	10kW	35kW	10kW	35kW	10kW	35kW
Pressure (kPa)	3.07	9.55	4.00	12.5	2.85	8.77
Void fraction	0.024	0.101	0.063	0.264	0.009	0.088
Coolant temperature (K)	0.341	1.63	1.13	3.15	0.225	1.52

`THM prototype` successfully predicts the coolant temperature in the $P_{tot} = 10$ and $35kW$ cases as depicted in Figure 4c. The axial evolution of the void fraction is also fairly satisfactory, especially when considering low power levels. It can be noted from Figure 4a that `THM prototype` consistently underestimates the void fraction in the lower parts of the core. On the other hand, the void fraction is over estimated in the upper section of the channel. This hints at the necessity to implement a sub-cooled boiling model to treat the initial bubble formation. Looking at Figure 4b it can be seen that the `THM prototype` fails to accurately predict the axial evolution of pressure, specifically in the $P_{tot} = 10kW$ case. Indeed, `THM prototype` pressure drop is over-estimated by a factor of 2. The cause of these discrepancies regarding pressure evolution is currently being investigated.

5. CONCLUSIONS

This work presents developments made at EPM towards the modeling of BWRs in the Version5 environment. The newly implemented **open-source** `THM prototype`, based on a drift flux model, is presented. It is coupled to the full core code DONJON5 through the *PyGan* interface. A single BWR pincell is modeled and studied as both an equivalent full core and coolant channel. The impact of the axial discretization and power normalization is assessed. An attempt at numerical validation is made by comparing to Serpent2 and GeN-Foam. The neutronics calculation is successfully validated with respect to Serpent2. However, the comparison between our `THM prototype` and GeN-Foam reveals that our drift-flux model fails to accurately predict axial variations in pressure. It also appears that our ebullition model could be improved, as the void fraction evolution is not entirely satisfactory when compared to GeN-Foam. This could be explained by the important differences between our homogeneous representation of the two-phase flow and the more elaborate CFD description implemented in GeN-Foam. Further work is needed to validate the `THM prototype` before it can be implemented in the open-source full core code DONJON5. Ongoing work involves validating `THM prototype` by studying the PSBT OECD/NEA benchmark, in addition to the ATRIUM-10-like assembly introduced in this work.

ACKNOWLEDGEMENTS

This work received support from the Natural Science and Engineering Research Council of Canada under grant ALLRP 586456-2023.

REFERENCES

[1] H. Okuno, Y. Naito, and Y. Ando. "OECD/NEA burnup credit criticality benchmarks phase IIIA: Criticality calculations of BWR spent fuel assemblies in storage and transport." Technical report, Japan Atomic Energy Research Institute (2000).

[2] A. Hebert. *Applied Reactor Physics*. Presses internationales Polytechnique (2009).

[3] A. Hébert. "Revisiting the simplified thermo-hydraulics module THM: in DONJON5 code." Technical report, Institut de génie nucléaire, Département de génie physique, Polytechnique Montréal (2018). Technical report IGE-409.

[4] A. Hébert. "DRAGON5 and DONJON5, the contribution of École Polytechnique de Montréal to the SALOME platform." *Annals of Nuclear Energy*, **volume 87**, pp. 12–20 (2016). Special Issue of The 3rd International Conference on Physics and Technology of Reactors and Application.

[5] J. Leppänen, M. Pusa, T. Viitanen, V. Valtavirta, and T. Kaltiaisenaho. "The Serpent Monte Carlo code: Status, development and applications in 2013." *Annals of Nuclear Energy*, **volume 82**, pp. 142–150 (2015). Joint International Conference on Supercomputing in Nuclear Applications and Monte Carlo 2013, SNA + MC 2013. Pluri- and Trans-disciplinarity, Towards New Modeling and Numerical Simulation Paradigms.

[6] C. Fiorina, I. Clifford, M. Aufiero, and K. Mikityuk. "GeN-Foam: a novel OpenFOAM® based multi-physics solver for 2D/3D transient analysis of nuclear reactors." *Nuclear Engineering and Design*, **volume 294**, pp. 24–37 (2015).

[7] M. Ishii and T. Hibiki. *Thermo-fluid dynamics of two-phase flow*. Springer Science and Business Media, New York, N.Y (2006).

[8] A. Wysocki, A. Ward, A. Manera, T. Downar, Y. Xu, J. March-Leuba, C. Thurston, N. Hudson, and A. Ireland. "The Modeling of Advanced Fuel Designs with the NRC Fuel Depletion Codes PARCS/PATHS." *Nuclear technology*, **volume 190**, pp. 323–335 (2015).

[9] NEA. *Physics of Plutonium Recycling*. OECD Publishing (2003).

[10] Advanced Reactors Information System ARIS. "Status Report – BWRX-300 (GE Hitachi and Hitachi GE Nuclear Energy) USA." Technical report, IAEA (2019).

[11] S. Radman, C. Fiorina, and A. Pautz. "Development of a novel two-phase flow solver for nuclear reactor analysis: Validation against sodium boiling experiments." *Nuclear Engineering and Design (Print)*, **volume 384**, p. 111422 (2021).

[12] A. Santamarina and N. Hfaiedh. "The SHEM energy mesh for accurate fuel depletion and BUC calculations." *Proceedings of ICNC2007* (2007).

[13] A. Hébert. "A General Formulation of the Resonance Spectrum Expansion Self-Shielding Method." *Nuclear Science and Engineering*, pp. 1–14 (2024).

[14] A. Hébert. "A User Guide For TRIVAC Version5." Technical report, Institut de génie nucléaire, Polytechnique Montréal (2023). TECHNICAL REPORT IGE–369.

[15] A. Hébert and R. Roy. "The GANLIB5 Kernel Guide (64–bit clean version)." Technical report, Institut de génie nucléaire, Département de génie mécanique, Polytechnique Montréal (2023). Technical report IGE–332.

[16] B. Massey and J. Ward-Smith. *Mechanics of Fluids*, volume 8. Taylor and Francis (2006).

[17] R. W. Lockhart and R. C. Martinelli. "Proposed correlation of data for isothermal two-phase two-component flow in pipes." *Chemical Engineering Progress 45* (1949).

[18] G. Marleau, A. Hébert, and R. Roy. "A User Guide For DRAGON Version5 ." Technical report, Institut de génie nucléaire Département de génie mécanique Ecole Polytechnique de Montréal (2024). TECHNICAL REPORT IGE–335.